

# Electric-field-induced phase transitions in rhombohedral $\text{Pb}(\text{Zn}_{1/3}\text{Nb}_{2/3})_{1-x}\text{Ti}_x\text{O}_3$

B. Noheda,\* Z. Zhong, D. E. Cox, and G. Shirane  
 Brookhaven National Laboratory, Upton, New York 11973

S-E. Park  
 Fraunhofer-IBMT Technology Center Hialeah, Hialeah, Florida 33010

P. Rehrig  
 Materials Research Laboratory, The Pennsylvania State University, University Park, Pennsylvania 16802  
 (Received 11 January 2002; published 22 May 2002)

High-energy x-ray-diffraction experiments performed on rhombohedral  $\text{Pb}(\text{Zn}_{1/3}\text{Nb}_{2/3})_{1-x}\text{Ti}_x\text{O}_3$  (PZN- $x\%$ PT) crystals with  $x=4.5\%$  and  $8\%$  show that an electric field applied along the [001] direction induces the tetragonal phase, as proposed by Park and Shrout. Our experiments reveal that in PZN-4.5%PT such a phase change occurs *via* a third phase with monoclinic symmetry  $M_A$ , which is observed at intermediate field values. This is in agreement with first-principles calculations by Fu and Cohen predicting the rotation of the polarization between the rhombohedral and tetragonal phases in this material. A different polarization path between the rhombohedral and tetragonal phases, through a second monoclinic phase  $M_C$ , has been previously reported in PZN-8%PT. The microscopic characterization of these crystals allows us to explain the ultrahigh macroscopic strain observed in PZN- $x\%$ PT under an electric field. Furthermore, some unusual scattering profiles displayed by exceptionally good crystals provide experimental evidence of the high anharmonicities and near degeneracy of the different phases in these extremely deformable materials.

DOI: 10.1103/PhysRevB.65.224101

PACS number(s): 77.65.-j, 61.10.Nz, 77.84.Dy

## I. INTRODUCTION

Piezoelectric single crystals of the relaxor-ferroelectric material  $\text{Pb}(\text{Zn}_{1/3}\text{Nb}_{2/3})_{1-x}\text{Ti}_x\text{O}_3$  (PZN- $x\%$ PT) oriented along an [001] direction show exceptionally large piezoelectric deformations, more than  $1\%$ .<sup>1,2</sup> In their pioneering work, Park and Shrout<sup>2</sup> proposed that the origin of the ultrahigh strain values observed in [001]-oriented PZN-8%PT (8PT) was a rhombohedral-to-tetragonal phase transition induced by the electric field. Later, Liu *et al.*<sup>3</sup> reported similar behavior in 4.5PT [see Fig. 1(a)]. A revolution in the world of piezoelectric devices seems certain to occur if the physical properties of such highly deformable materials can be understood and controlled.

Diffraction experiments on 8PT under an applied [001] field have revealed the true long-range symmetry evolution to be from a rhombohedral to a monoclinic phase.<sup>4</sup> These measurements were performed on relatively thick samples, and a single tetragonal phase could not be reached before sample breakdown [see Fig. 1(b)]. However it was shown that it is the existence of such a monoclinic phase, rather than a tetragonal one, which is crucial in explaining the outstanding properties of these materials.

Monoclinic phases have been observed in the temperature-composition phase diagrams of three of the most important piezoelectric systems,  $\text{Pb}(\text{Zr}_{1-x}\text{Ti}_x)\text{O}_3$  (PZT),<sup>5</sup> PZN- $x\%$ PT,<sup>6-8</sup> and very recently also in  $\text{Pb}(\text{Mg}_{1/3}\text{Nb}_{2/3})_{1-x}\text{Ti}_x\text{O}_3$  (PMN-PT),<sup>9-12</sup> for compositions around the morphotropic phase boundary (MPB), which represents the nearly vertical limit between the rhombohedral and the tetragonal phases. Furthermore, it has been observed that the region of stability of those phases is enlarged following the application of an electric field.<sup>4,13,14</sup> Optical<sup>15</sup> and

x-ray-diffraction<sup>16,17</sup> measurements have also indicated a symmetry lowering in poled 8PT.

In contrast to the rhombohedral or tetragonal phases, the polarization vectors in the monoclinic phases are no longer constrained to be directed along a symmetry axis and can rotate within the monoclinic plane. However, different polarization rotation paths have been observed in these materials, resulting in two types of monoclinic distortion  $M_A$  (as found in PZT) and  $M_C$  (as found in 8PT) with space groups  $Cm$  and  $Pm$ , respectively. As illustrated in Fig. 1(c), in the  $M_A$  type, the monoclinic plane is the pseudocubic (110) plane and the unit cell is doubled in volume with respect to the  $4\text{-\AA}$  pseudocubic unit cell. In the  $M_C$  type, the unit cell is primitive and the monoclinic plane is the pseudocubic (010) plane. Very recently, Vanderbilt and Cohen<sup>18</sup> reported a natural derivation of these monoclinic phases by extending the Devonshire expansion of the free energy up to eighth-order, which is indicative of the large anharmonicity intrinsic to these highly piezoelectric materials. In what follows, we will use their notation for the various phases. A strong anharmonicity of the potential surfaces in lead oxides has also been proposed by Kiat *et al.*<sup>19</sup> based on experimental observations.

First-principles calculations by Bellaiche *et al.* have succeeded in reproducing the monoclinic phase in PZT, both at zero electric field<sup>20</sup> and also under an applied field.<sup>21</sup> Most importantly, the calculations have shown that the huge increase in the piezoelectric coefficients close to the MPB of these materials is directly related to polarization rotation between the rhombohedral [111] and tetragonal [001] polar axes<sup>22</sup> and, ultimately, to the existence of a monoclinic phase.<sup>20</sup> This has very important consequences for a fundamental understanding of the piezoelectric properties in these compounds.

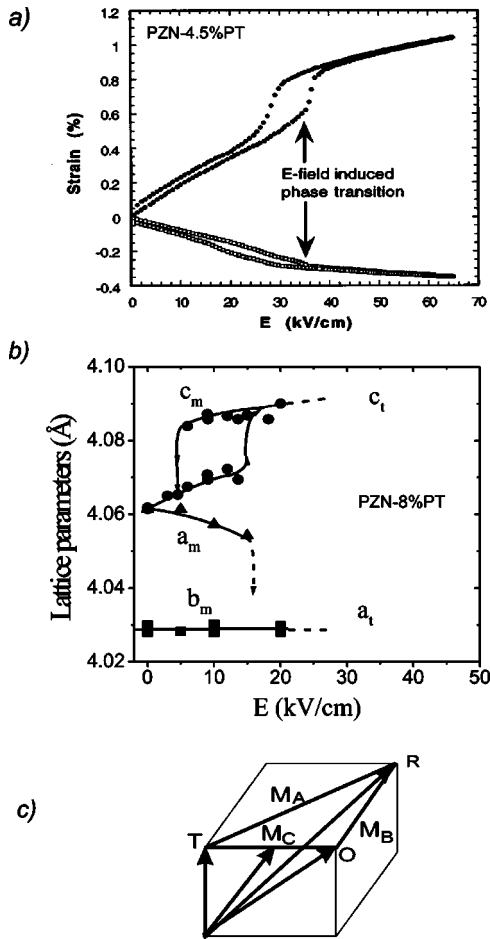


FIG. 1. (a) Macroscopic strain vs electric field for 4.5PT following Ref. 3. (b) Lattice parameters vs electric field for 8PT, adapted from Ref. 4. (c) Polarization vectors in the perovskite unit cell, shown by thick arrows. The thick lines represent the paths followed by the end of the polarization vector in the monoclinic phases, in between the rhombohedral ( $R$ ), tetragonal ( $T$ ), and orthorhombic ( $O$ ) phases. The  $M_A$ ,  $M_B$ ,  $M_C$  notation is adopted following Vanderbilt and Cohen (Ref. 18).

In this revealing context, a detailed interpretation of the various observations is required, with the goal of making the high-strain piezoelectric systems as controllable and convenient as the PZT-based materials in current use. We have accordingly performed high-energy x-ray-diffraction experiments on rhombohedral 4.5PT and 8PT crystals with an electric field applied *in situ* along the  $[001]$  direction, and studied how the symmetry evolves. A field-induced long-range tetragonal phase has in fact been observed in both 4.5PT and 8PT compositions, thus confirming Park and Shrout's hypothesis.<sup>2</sup> These experiments, together with those recently reported for 8PT,<sup>4,17,14</sup> 9PT,<sup>6,7</sup> and  $x$ PT ( $x \geq 10\%$ ),<sup>8</sup> provide a much clearer picture of the field-induced behavior in rhombohedral PZN- $x$ %PT. This work also provides the link between the anomalous macroscopic strain values in these materials and the evolution of the structural parameter under an applied field.

## II. EXPERIMENT

4.5PT and 8PT samples were grown by the high-temperature flux technique described in Ref. 2. The samples were then oriented and cut in the form of rectangular parallelepipeds, with sides ranging from 0.5 to 3 mm, and at least two of the faces perpendicular to an  $[001]$  direction. Gold was sputtered on two of the  $\{001\}$  faces of all the samples, and thin wires were attached to enable an electric field to be applied along the  $[001]$  direction. It should be noted that rhombohedral as-grown PZN- $x$ %PT crystals have a relaxor character and are, therefore, crystallographically disordered. In order to induce the ferroelectric long-range ordered state it is necessary to pole them under an electric field. This poling is typically accomplished by applying a field of about 10 kV/cm at room temperature. If the electric field is applied along the  $[111]$  direction, no change of symmetry is observed and the crystal in the ordered state is still rhombohedral. As described above, in this work the crystals are poled along the  $[001]$  direction. Very narrow mosaics were observed in the diffraction patterns demonstrating the excellent quality of the crystals.

Single-crystal diffraction experiments were carried out at the National Synchrotron Light Source, on beam lines X17B1 and X22A, with high-energy x rays of 67 keV ( $\sim 0.18$  Å) and 32 keV ( $\sim 0.38$  Å), respectively. High-energy x rays are needed to observe the crystal structure underneath the *skin* of the sample, which extends a few microns below the surfaces<sup>4,23</sup> and behaves differently from the bulk, as shown by Ohwada *et al.*<sup>14</sup> At X17B1, the high-flux monochromatic beam was obtained from a superconducting wiggler device by use of a Si(220) crystal in Laue-Bragg geometry. At X22A, the third-order reflection of a Si(111) monochromator crystal was used to provide the 32-keV beam. Both beamlines are equipped with four-circle Huber diffractometers, with Si(220) and Si(111) analyzer crystals mounted in the diffraction path at X17B1 and X22A, respectively.

For the diffraction experiments with an *in situ* electric field applied, a special sample holder was constructed in which the sample wires were soldered to the high-voltage leads, and the samples were unclamped and free to deform. The samples were coated with a silicone dielectric compound (*GC Electronics-type Z5*) to prevent arcing, and were kept in place with a tiny dab of vacuum grease. The maximum value of the applied field was limited by the dielectric breakdown of the samples; in the case of the thinnest samples ( $d=0.5$  mm), fields as high as 45 kV/cm were achieved.

## III. RESULTS

Three 4.5PT crystals ( $A$ ,  $B$ , and  $C$ ) were studied. In crystals  $A$  and  $B$  the monoclinic phase was unambiguously observed for  $E < 30$  kV/cm, consistent with the macroscopic strain measurements shown in Fig. 1(a).<sup>2</sup> The results obtained for crystal  $A$  are summarized in Fig. 2. The initial state at  $E=0$ , for which  $a_m/\sqrt{2} > c_m > b_m/\sqrt{2}$ , corresponds to a

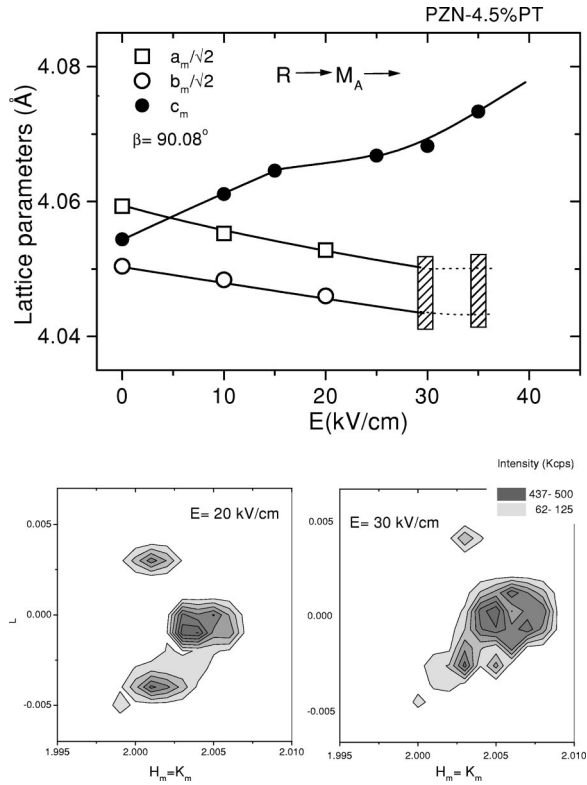


FIG. 2. Evolution of lattice parameters with an electric field applied along the [001] direction in a 4.5PT crystal (dimensions  $3 \times 3 \times 1$  mm<sup>3</sup>) in the rhombohedral and monoclinic phases, as observed by high-energy x-ray diffraction (top). Mesh scans in the *HHL* zone of reciprocal space around the pseudocubic (220) reflection are shown in the bottom plots for  $E = 20$  kV/cm (bottom left) and  $E = 30$  kV/cm (bottom right). Intensities are on a linear scale.

rhombohedral phase with  $a_r = 4.055$  Å and  $\alpha_r = 89.9^\circ$ .<sup>24</sup> Under the application of an electric field along the [001] direction, a monoclinic phase of  $M_A$  type is induced for  $E < 30$  kV/cm, as shown by a steady decrease in  $a_m/\sqrt{2}$  and  $b_m/\sqrt{2}$  and a corresponding increase in  $c_m$  (Fig. 2, top), and by a mesh scan in the reciprocal *HHL* plane (the monoclinic plane) around the pseudocubic (220) reflection at  $E = 20$  kV/cm (Fig. 2, bottom left). This monoclinic phase is similar to that observed in PZT,<sup>5</sup> in which  $a_m$  and  $b_m$  are rotated  $45^\circ$  about the pseudocubic [001] direction and are approximately equal to  $a_o\sqrt{2}$  and  $c_m \sim a_o$ , where  $a_o$  is the pseudocubic lattice parameter. The intensity distribution observed at 20 kV/cm in Fig. 2 (bottom left) arises from the presence of four different  $M_A$  domains formed when the field is applied along the [001] direction, as previously explained in Ref. 10. Peaks are observed at two different positions along the longitudinal scans around  $H = K = 2$ , corresponding to  $a_m$  and  $b_m$  respectively. The splitting between the pair of peaks at the smaller value of  $H = K$  (i.e., the larger lattice parameter  $a_m$ ) along the transverse (field) direction is related to the monoclinic angle  $\beta = 90.08^\circ$ . For  $E = 30$  kV/cm, the mesh scans have a more complicated appearance in that most of the intensity has coalesced within a single broad region, but with a distribution of lattice parameters (Fig. 2, bottom right), which we interpret as an incomplete transformation to

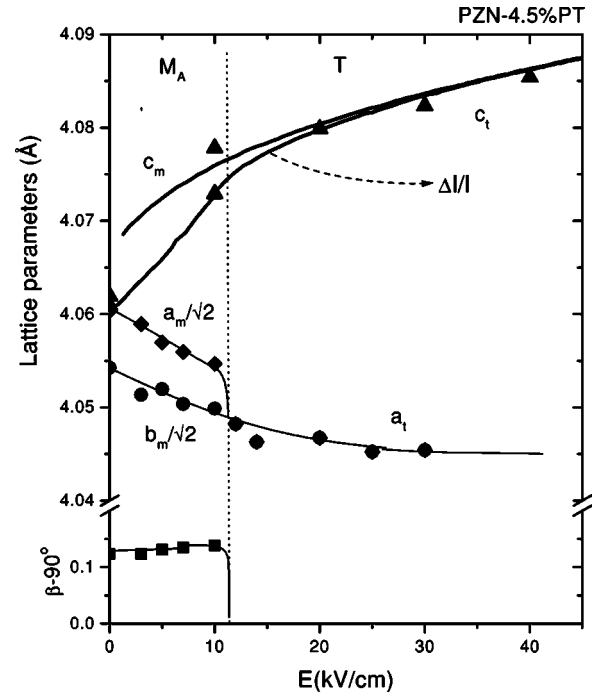


FIG. 3. Evolution of lattice parameters with an electric field applied along the [001] direction in the second 4.5PT crystal in the monoclinic and tetragonal phases, as observed by high-energy x-ray diffraction. The thick lines represent the macroscopic unipolar strain along the [001] direction obtained by dilatometric measurements on the same sample. The thinner lines are a guide to the eye.

a tetragonal phase. However, even at  $E = 35$  kV/cm, we did not observe a single tetragonal phase, probably because of the existence of several regions with different transformation fields.

The results obtained for crystal *C* were rather different, they showed unambiguously a crossover between the monoclinic and tetragonal phases, but at an anomalously low value of  $\sim 11$  kV/cm for this composition. The evolution of the lattice parameters under a [001] electric field for this crystal is shown in Fig. 3. In this case, the tetragonal phase, characterized by two lattice parameters  $a_t$  and  $c_t$ , is indeed observed at high fields, as proposed by Park and Shrout on the basis of macroscopic measurements.<sup>2</sup> When the field is decreased, the tetragonal distortion  $c_t/a_t$  also decreases; however, the tetragonal phase does not transform directly into a rhombohedral phase at low fields. Instead, a monoclinic phase is observed as  $a_t$  splits into  $a_m$  and  $b_m$ , and the angle  $\beta$  between  $a_m$  and  $c_m$  becomes slightly greater than  $90^\circ$ . This monoclinic phase is also of  $M_A$  type, and as can be seen in Fig. 3, the crystal remains monoclinic even at  $E = 0$ . It is noteworthy that at this point,  $c_m \sim a_m/\sqrt{2}$ , corresponding to the singular case of a monoclinic cell with the polarization vector lying along the rhombohedral polar axis [111], probably as a result of the underlying monoclinic distortion of the oxygen octahedra. In order to recover the initial rhombohedral phase, it would be necessary to apply a field in the reverse direction.

Figure 4 shows the region of the reciprocal *HHL* plane around the pseudocubic (330) reflection for several different

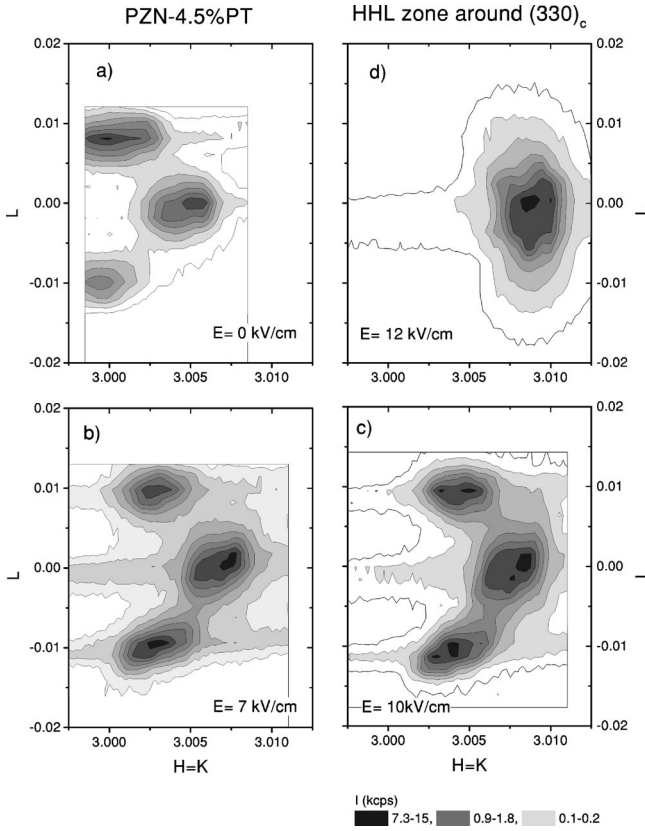


FIG. 4. Mesh scans around the pseudocubic (330) reflection in the *HHL* zone of the reciprocal space for the second crystal of 4.5PT at  $E=0$  (a), 7 (b), 10 (c), and 12 (d) kV/cm. The intensities are plotted on a logarithmic scale.

values of  $E$ . The intensity distributions observed in Figs. 4(a)–4(c) ( $E=0$ , 7, and 10 kV/cm, respectively) arise from the four different  $M_A$  monoclinic domains formed when the field is applied along the [001] direction, as noted previously. Once again, peaks are observed at two different positions along the longitudinal scans around  $H=K=3$ , corresponding to  $a_m$  and  $b_m$ , respectively. Note that  $H=K=L=3$  is defined in order to reflect the value of  $c_m$  at  $E=0$ , so that the value  $H=K=3$  in the scans means that  $a_m=c_m$ . The splitting between the pair of peaks at the smaller value of  $H=K$  corresponds to a monoclinic angle of  $\beta=90.13^\circ$ . As the field is increased, both  $a_m$  and  $b_m$  decrease, as shown by the shifts to larger  $H=K$  values. At  $E=12$  kV/cm, the intensity has coalesced into a single peak [Fig. 4(d)] and the crystal is in the tetragonal phase (i.e.,  $a_m=b_m$ ,  $\beta=90^\circ$ ). From Fig. 3, it is seen that the transformation occurs at about 11 kV/cm. The composition of the crystal  $C$  was confirmed using dielectric measurement, with  $T_{max}$  being  $170^\circ\text{C}$ . In addition to the exceptionally low phase-transition field, the strain behavior associated with the phase transition in Fig. 3 does not show the typical hysteretic jump at the transition field. We suspect that the defect structure and subsequent abnormal domain configuration may affect the phase-transition behavior of this crystal. Further investigation is going on.

4.5PT, therefore, behaves differently than 8PT, as can be readily inferred from Fig. 1(b). As reported in Ref. 4, application of a [001] electric field to the latter yields a mono-

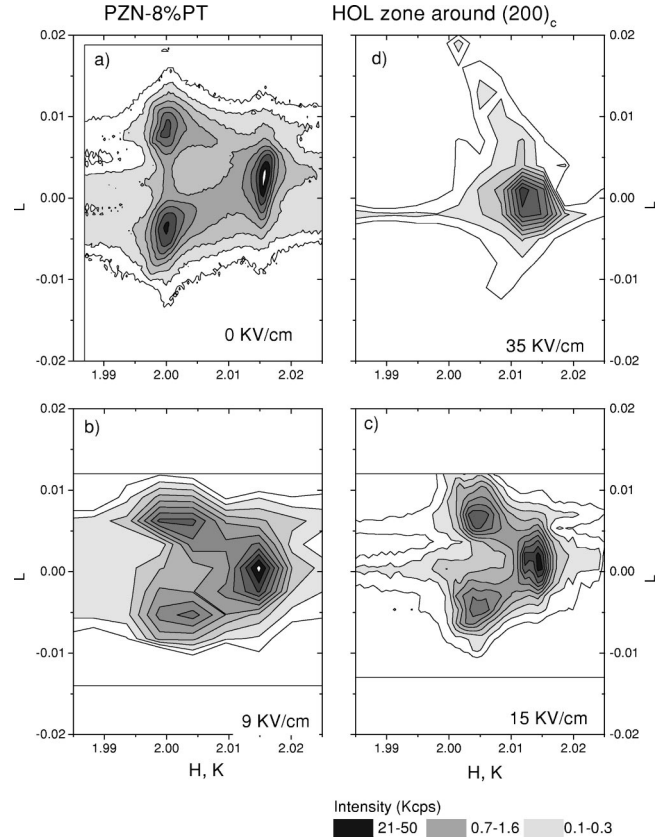


FIG. 5. Mesh scans around the pseudocubic (200) reflection in the *HOL* (or *OKL*) zone of reciprocal space for 8PT at  $E=0$  (a), 9 (b), 15 (c), and 35 (d) kV/cm. The intensities are plotted on a logarithmic scale.

clinic cell of  $M_C$  type, with a primitive cell of about  $4 \text{ \AA}$  along the edge. In the 8PT case the characteristic intensity distribution resulting from the four possible monoclinic domains is observed in the *OKL* (or *HOL*) zone of reciprocal space, since the monoclinic angle is now contained within the (010) plane. Figures 5(a)–5(d) show such intensity distributions around the pseudocubic (200) reflection for several different values of the applied electric field  $E=0$ , 9, 15, and 35 kV/cm, respectively. Unlike 4.5PT,  $b_m$  remains approximately constant at  $K=2.015$  as the field is increased, while  $a_m$  decreases, approaching  $b_m$  [see also Fig. 1(b)]. At sufficiently high fields,  $a_m$  becomes equal to  $b_m$  and the crystal becomes tetragonal, showing a single reflection around the (200) point in reciprocal space [Fig. 5(d)], as also illustrated by the dotted lines in Fig. 1(b).

When the field is removed, the crystal does not become rhombohedral, but resembles 4.5PT in this respect, with  $a_m=c_m \neq b_m$ ,  $\beta \neq 90^\circ$ . However, unlike  $M_A$ , in this case the equality  $a_m=c_m$  corresponds to a higher symmetry than  $M_C$ , namely, orthorhombic,  $O$  [see also Fig. 1(c)].<sup>5</sup> This “pseudomonoclinic”  $O$  phase ( $O^*$ ) has recently been observed in the phase diagram of PZN- $x$ %PT for 9PT and 10PT.<sup>6–8</sup>

As we have mentioned, the crossover between the monoclinic and tetragonal phases depends on the sample composition, as well as on the experimental conditions, such as

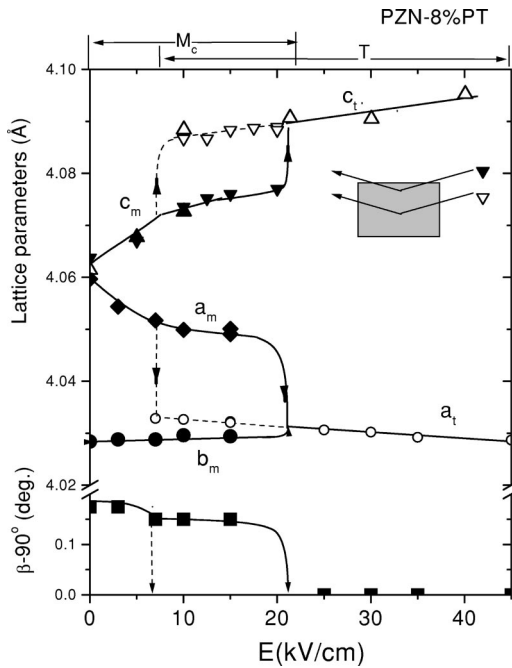


FIG. 6. Evolution of lattice parameters with an electric field applied along the [001] direction for a 8PT crystal. Solid symbols represent the monoclinic lattice parameters. Open symbols represent the tetragonal lattice parameters. Inverted triangles show the results of measurements of the  $c$  parameter with a 100- $\mu\text{m}$  beam at two different depths in the crystal, as illustrated schematically in the inset.

mechanical clamping. High-energy x-ray diffraction has revealed that the critical fields at which the monoclinic-to-tetragonal phase change takes place are different across the sample thickness,<sup>14</sup> most likely due to a distribution of strain. Figure 6 shows the lattice parameters of one of the 8PT crystals under an [001] electric field. The results are very similar to those in Fig. 1(b) (Ref. 4) but in this case the tetragonal phase could be reached. We observed an intermediate region ( $7 < E < 20$  kV/cm) in which the two phases, monoclinic  $M_C$  and tetragonal, coexist. Measurements of the  $c$  lattice parameter made with a narrow beam about 100  $\mu\text{m}$  in width (inverted triangles in Fig. 6) showed that the tetragonal phase was indeed reached at different field values across the sample thickness, between 7–20 kV/cm.

#### IV. DISCUSSION

The most outstanding feature of the [001]-oriented rhombohedral PZN- $x\%$  PT crystals is the extremely high deformation that can be obtained under the application of an electric field. Of paramount interest from the applications point of view is the fact that large elongations can be obtained with very little hysteresis, which means virtually no domain-wall motion. As observed in the  $\Delta l/l$  measurements plotted in Fig. 3, the macroscopic deformation of about 0.6% in 4.5PT for  $E \leq 40$  kV/cm corresponds very closely to the elongation of the unit cell along the field direction. The observed total strain is due partly to polarization rotation and elongation in the  $M_A$  phase between [111] and [001] and partly due to the

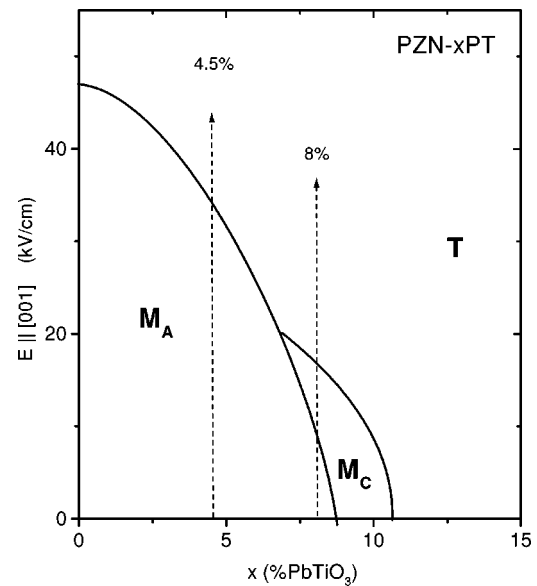


FIG. 7. Sketch of the [001] electric field vs composition phase diagram for PZN- $x\%$  PT.

$c$ -axis elongation of the unit cell in the tetragonal phase. However, a change of slope is clearly observed in both  $\Delta l/l$  and the  $c$  parameter with applied field at the  $M_A$ - $T$  phase transition, from which it can be inferred directly that the piezoelectric modulus (elongation per volt) in the monoclinic phase is about five times larger than that in the tetragonal phase.

The observed macroscopic strain depends on the initial domain configuration, and thus, on the previous history of the crystal. The coincidence of the microscopic and macroscopic measurements in Fig. 2 indicates that the crystal consisted only of domains with polarizations  $35^\circ$  away from the field direction [001] (see Refs. 2 and 25). When the field is applied, the polarization of the domains rotates until the crystal becomes tetragonal and monodomain, with the polarization parallel to the field.

However, a negative electric field or mechanical pressure along the field direction can favor domains with polarizations closer to the plane perpendicular to the field, as recently described for the PZT case.<sup>26</sup> This fact can explain the dramatic differences observed between the stress-free-bipolar and slightly-clamped-unipolar strain curves reported by Viehland<sup>17</sup> on 8PT crystals. The deep strain level of  $-0.6\%$  and the aggregate strain level of  $1.2\%$  observed in the bipolar strain curve of [001]-oriented 8PT crystals correspond to the maximum spontaneous strain observed for  $M_C$ , i.e., the strain between the monoclinic  $a$  and  $b$ , and  $b$  and  $c$  axes, respectively [see Fig. 1(b)].

The extreme sensitivity of these materials to the experimental conditions, in particular, to stress is an indication of the near degeneracy of the different phases around their MPB's. Although the exact field values at which the phase transitions happen would need to be determined for very specific experimental conditions, we still can sketch an electric field vs composition phase diagram for rhombohedral PZN- $x\%$  PT as shown in Fig. 7. Close to the MPB at 8PT, the

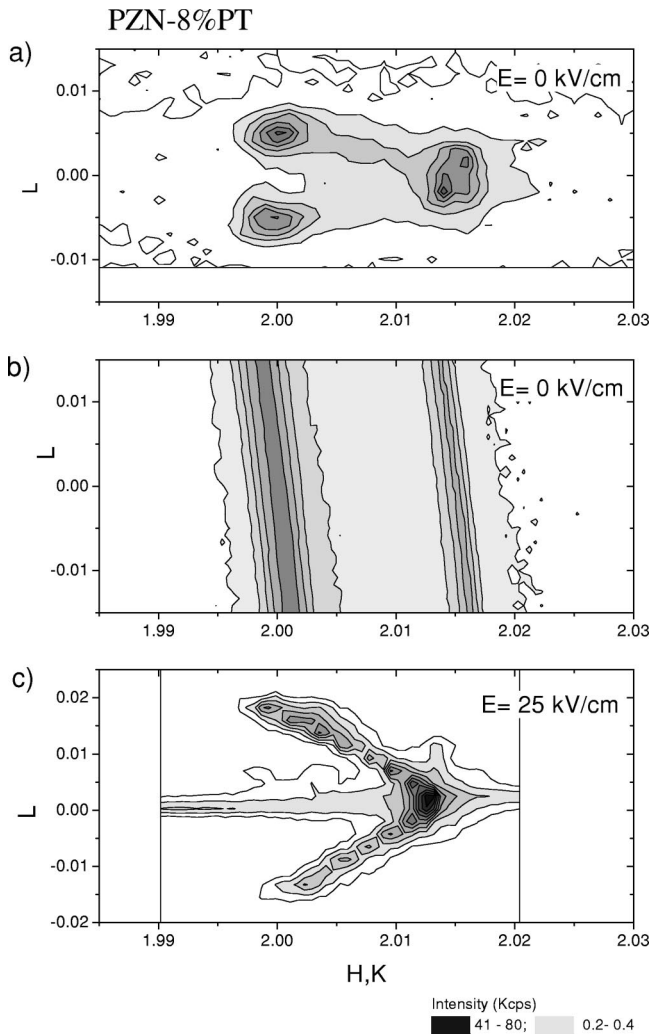


FIG. 8. (a) Typical profile observed for 8PT in the  $HOL$  zone of reciprocal space around the pseudocubic (200) reflection at  $E=0$ . (b) Example of an unusual profile observed in the same region. (c) An unusual intensity distribution observed for the same composition in the tetragonal phase. The intensities are on a logarithmic scale.

$M_A$  phase is only stable at very low fields,<sup>14</sup> while no  $M_C$  phase has been so far observed for 4.5PT.

An intricate and history-dependent domain configuration is another consequence of the high degeneracy of the various phases displayed by the PZN- $x$ PT system, which can also produce some exotic and unusual diffraction intensity distributions, especially for compositions very close to the MPB. Figure 8(a) shows the three-peak pattern usually observed in 8PT crystals in the  $HOL$  zone around the pseudocubic (200) reflection at  $E=0$ , arising from the four different monoclinic domains.<sup>4</sup> However, on one occasion a very interesting rod-

like intensity distribution was observed in the same crystal upon the removal of the electric field [Fig. 8(b)], the  $d$  spacings of the rods being identical to those of the Bragg peaks. Unfortunately, we were never able to reproduce such a rod pattern, but we speculate that this interesting behavior may be due to a complicated domain formation. Another example of unusual diffuse scattering is shown in Fig. 8(c), corresponding to the same region of the reciprocal space of a 8PT crystal under a 25 kV/cm [001] electric field. Most of the crystal has transformed into the tetragonal phase characterized by a single lattice parameter in this zone [as in Fig. 5(d)]. The sharpness of this reflection shows the excellent quality of the crystal and the accuracy of the electric-field orientation. However, when plotted on a logarithmic scale [as in Fig. 8(c)], a fascinating fishlike shape is revealed, indicating that a small fraction of the sample retains a distribution of both lattice parameters and monoclinic angles.

To conclude, the polarization rotation path has been investigated for rhombohedral 4.5PT and 8PT single crystals under a [001] electric field. In 4.5PT the polarization vector rotates directly from [111] towards [001] via a monoclinic  $M_A$  phase. In 8PT, which lies closer to the MPB, the polarization vector jumps at a relatively low field to the (010) plane and rotates in this plane, via a monoclinic  $M_C$  phase, towards [001] when the field is increased.<sup>4</sup> For both compositions a single tetragonal phase has been observed at high fields. The behavior of the lattice parameters as a function of electric field can account for the ultrahigh macroscopic piezoelectric deformations in terms of the microscopic deformation of the unit cell (rotation plus elongation).

On occasions, unique contour plots have been recorded, especially for the 8PT crystals, which show very peculiar intensity distributions and are believed to reflect the existence of heavily twinned materials and complicated local effects. Further work is needed to fully understand some of these features; in particular, a detailed study of the complicated diffuse scattering would provide very useful information about the local order in these materials. However, we may safely conclude that all the reported observations are consequences of the high anharmonicity and the delicate energy balance between the different phases in these highly deformable materials.

## ACKNOWLEDGMENTS

Stimulating discussions with G. Baldinozzi, L. Bellaiche, L.E. Cross, B. Dkhil, M. Durbin, K. Hirota, K. Ohwada, J-M. Kiat, D. Vanderbilt, D. Viehland, and T. Vogt, as well as the technical support of A. Langhorn are gratefully acknowledged. Financial support by DOE under Contract No. DE-AC02-98CH10886 and the Office of Naval Research is also acknowledged.

\*Corresponding author. Present address: Condensed Matter Physics, Vrije Universiteit, De Boelelaan 1081, 1081 HV Amsterdam, The Netherlands. Email address: noheda@nat.vu.nl

<sup>1</sup>J. Kuwata, K. Uchino, and S. Nomura, Jpn. J. Appl. Phys., Part 1 **21**, 1298 (1982).

<sup>2</sup>S-E. Park and T.R. Shrout, J. Appl. Phys. **82**, 1804 (1997).

<sup>3</sup>S-F. Liu, S-E. Park, T. Shrout, and L.E. Cross, J. Appl. Phys. **85**, 2810 (1999).

<sup>4</sup>B. Noheda, D.E. Cox, G. Shirane, S-E. Park, L.E. Cross, and Z. Zhong, Phys. Rev. Lett. **86**, 3891 (2001).

- <sup>5</sup>B. Noheda, D.E. Cox, G. Shirane, J.A. Gonzalo, L.E. Cross, and S-E. Park, *Appl. Phys. Lett.* **74**, 2059 (1999); B. Noheda, J.A. Gonzalo, L.E. Cross, R. Guo, S-E. Park, D.E. Cox, and G. Shirane, *Phys. Rev. B* **61**, 8687 (2000); B. Noheda, D.E. Cox, G. Shirane, R. Guo, B. Jones, and L.E. Cross, *ibid.* **63**, 014103 (2001).
- <sup>6</sup>D.E. Cox, B. Noheda, G. Shirane, Y. Uesu, K. Fujishiro, and Y. Yamada, *Appl. Phys. Lett.* **79**, 400 (2001).
- <sup>7</sup>Y. Uesu, M. Matsuda, Y. Yamada, K. Fujishiro, D. E. Cox, B. Noheda, and G. Shirane, *J. Phys. Soc. Jpn.* **71**, 960 (2002).
- <sup>8</sup>D. La-Orautapong, B. Noheda, Z-G. Ye, P.M. Gehring, J. Toulouse, D.E. Cox, and G. Shirane, *Phys. Rev. B* **65**, 144101 (2002).
- <sup>9</sup>G. Xu, H. Luo, H. Xu, and Z. Yin, *Phys. Rev. B* **64**, 020102 (2001).
- <sup>10</sup>Z-G. Ye, B. Noheda, M. Dong, D.E. Cox, and G. Shirane, *Phys. Rev. B* **64**, 184114 (2001).
- <sup>11</sup>J.-M. Kiat, Y. Uesu, B. Dkhil, M. Matsuda, C. Malibert, and G. Calvarin, *Phys. Rev. B* **65**, 064106 (2002).
- <sup>12</sup>A.K. Singh and D. Pandey, *J. Phys.: Condens. Matter* **13**, L931 (2001).
- <sup>13</sup>R. Guo, L.E. Cross, S-E. Park, B. Noheda, D.E. Cox, and G. Shirane, *Phys. Rev. Lett.* **84**, 5423 (2000).
- <sup>14</sup>K. Ohwada, K. Hirota, P.W. Rehrig, P.M. Gehring, B. Noheda, Y. Fujii, S-E. Park, and G. Shirane, *J. Phys. Soc. Jpn.* **70**, 2778 (2001).
- <sup>15</sup>D-S. Paik, S-E. Park, S. Wada, S-F. Liu, and T. Shrout, *J. Appl. Phys.* **85**, 1080 (1999).
- <sup>16</sup>M.K. Durbin, J.C. Hicks, S.-E. Park, and T.R. Shrout, *J. Appl. Phys.* **87**, 8159 (2000).
- <sup>17</sup>D. Viehland, *J. Appl. Phys.* **88**, 4794 (2000); D. Viehland, J. Powers, and L. Ewart, *ibid.* **88**, 4907 (2000).
- <sup>18</sup>D. Vanderbilt and M.H. Cohen, *Phys. Rev. B* **63**, 094108 (2001).
- <sup>19</sup>J-M. Kiat, G. Baldinozzi, M. Dunlop, C. Malibert, B. Dkhil, C. Menoret, O. Masson, and M.T. Fernandez-Diaz, *J. Phys.: Condens. Matter* **12**, 8411 (2000).
- <sup>20</sup>L. Bellaiche, A. Garcia, and D. Vanderbilt, *Phys. Rev. Lett.* **84**, 5427 (2000).
- <sup>21</sup>L. Bellaiche, A. Garcia, and D. Vanderbilt, *Phys. Rev. B* **64**, 060103(R) (2001).
- <sup>22</sup>H. Fu and R.E. Cohen, *Nature (London)* **403**, 281 (2000).
- <sup>23</sup>B. Noheda, D. E. Cox, and G. Shirane, cond-mat/0109545, *Ferroelectrics* (to be published).
- <sup>24</sup>It can be easily shown that in the rhombohedral phase,  $a_m$ ,  $b_m$ , and  $c_m$  are no longer independent, and are related to the rhombohedral lattice parameters  $a_r$  and  $\alpha_r$  as follows:  $a_m = 2a_r \cos(\alpha_r/2)$ ,  $b_m = 2a_r \sin(\alpha_r/2)$ , and  $c_m = a_r$ . The monoclinic angle  $\beta$  is then defined as  $180^\circ - \phi$ , where  $\cos(\phi) = [1 - 2 \sin^2(\alpha_r/2)] / \cos(\alpha_r/2)$ .
- <sup>25</sup>L.E. Cross, in *Fundamental Physics of Ferroelectrics 2000*, edited by Ronald E. Cohen, AIP Conf. Proc. 535 (AIP, Melville, NY, 2000), pp. 1–15.
- <sup>26</sup>P. Chaplya and G.P. Carman, *J. Appl. Phys.* **90**, 5278 (2001).